Change of Diffusion Mechanism with Lattice Parameter in the Series of Lanthanide Indides Having $L1_2$ Structure

Gary S. Collins, Xia Jiang, John P. Bevington, and Farida Selim
Department of Physics and Astronomy, Washington State University, Pullman, Washington 99164, USA

Matthew O. Zacate
Department of Physics, Northern Kentucky University, Highland Heights, Kentucky 41099, USA
(Received 6 October 2008; published 17 April 2009)

Using perturbed angular correlation spectroscopy, jump frequencies of Cd tracer atoms were measured for 12 indides In_3B (B = rare earth) in paired samples having compositions at each of the opposing phase boundaries. Jump frequencies in heavy lanthanide indides were observed to be smaller for In-richer compositions than for In-poorer compositions, but greater in the light lanthanide indides. These findings signal an unmistakable change in diffusion mechanism from the simple In-sublattice vacancy mechanism for heavy lanthanides to a B-vacancy mechanism for light lanthanides.

DOI: 10.1103/PhysRevLett.102.155901 PACS numbers: 66.30.−h, 76.80.+y, 82.80.Ej

There is increasing interest in diffusion mechanisms in complex crystal structures [1,2]. Traditionally, diffusion has been studied by direct observation of mass transport, e.g., penetration of tracer atoms into a substrate. Insight into mechanisms has come by observing how the diffusivity varies, e.g., with isotopic mass, pressure, or composition [1]. Recently developed methods provide direct information about atomic scale processes. For example, quasielastic neutron scattering in single crystals has been used to determine elementary jump vectors in the crystal structure and thereby discriminate between near-neighbor and next-near-neighbor jumps [3]. Jump frequencies of a diffusing species can be measured by mechanical relaxation or nuclear hyperfine interaction methods such as nuclear magnetic resonance (NMR) and the Mössbauer effect [1]. In cubic structures, the diffusivity D is related to the jump distance ℓ and jump-frequency w via $D = \frac{1}{6} f \ell^2 w$, in which f is a correlation coefficient of diffusion [4]. w is defined here as the inverse of the mean residence time of an atom at a site.

Recently, two of us applied perturbed angular correlation spectroscopy (PAC) to measure jump frequencies of probe atoms in compounds. First measurements were on In_3La [5], which has the cubic $L1_2$, or Cu_3Au, structure. The In-sites have tetragonal point symmetry with axes pointing along the three cube directions and axially symmetric electric field gradients (EFG). We used the well-known radioactive ^{111}In probe that decays by gamma-gamma emission through the long-lived, 247 keV, spin 5/2 level of ^{111}Cd. In the absence of diffusional jumps, Cd daughter nuclei experience a static nuclear quadrupole interaction due to the EFGs at the In-sites. The interaction is detected as spin precessions in the time domain. The geometry of the In-sublattice has the special feature that the principal axis of the EFG tensor reorients by 90° in each near-neighbor (NN) jump, leading to decoherence of the quadrupolar precessions. Initial measurements on In_3La were followed by studies on several other rare-earth indides [6] and stannides [7].

We refer to the $L1_2$ phases as A_3B phases below, with A = indium and B = rare earth. All such phases appear as ''line compounds'' in binary phase diagrams of indium and rare-earth elements [8], meaning that widths of the $L1_2$ phase fields are narrower than the typical resolution of about 1 at. % in conventional metallurgical phase analysis. Narrow field widths imply high formation enthalpies for point defects and, consequently, excellent ordering of elements on their respective sublattices. Internal evidence for a high degree of order in the phases comes from the PAC measurements themselves, since none of the spectra observed in the previous or present measurements exhibited significant inhomogeneous broadening near ambient temperatures. We estimate that each boundary composition lies within about 0.2 at. % of the stoichiometric composition.

In the past and present work, we studied pairs of samples prepared to have compositions of the opposing boundary compositions. Jump frequencies measured for the two boundary compositions were found to differ by factors up to 100 [5–7]. As prepared, samples consist mostly of the $L1_2$ phase, with minor volume fractions of adjacent phases, either In-metal for A-richer boundary compositions or one of several kinds of B-richer intermediate phases for B-richer compositions. In the earlier work, the jump frequency was found to be greater for A-richer In_3La [5] but greater for B-richer Sn_3La [6]. The present study was undertaken to shed light on this difference through measurements of jump frequencies on a comprehensive set of $L1_2$ rare-earth indides. As will be shown, the jump frequency gradually crosses over from being greater at the B-richer boundary composition for indides of heavy lanthanides to being greater at the A-richer boundary for the

light lanthanides. As discussed below, this indicates a change in the predominant diffusion mechanism along the series.

Samples were made by melting 99.9 at. % pure rare-earth elements, 99.999 at. % indium, and carrier-free ^{111}In activity under argon. Arc-melting takes about 1 s and results in a ~30–60 mg spherical alloy sample. The mole fraction of ^{111}In is about 10^{-8}. The sample is transferred to a PAC oven within minutes and measurements are made over 1–2 weeks in vacuum under a pressure of about 10^{-6} Pa. Sample compositions were determined by measuring the masses of the constituent metals before melting. Uncertainties in composition were calculated by taking into account any mass loss during the melt. Sample compositions were well within two-phase fields, guaranteeing that compositions of the $L1_2$ phases were at the targeted phase boundaries.

PAC perturbation functions $G_2(t)$ were measured at temperatures up to ~1250 °C using a four-detector spectrometer. All measurements reported here were made in the slow fluctuation regime, in which the jump frequency w is less than the quadrupole interaction frequency. Experimental PAC perturbation functions were fitted using the approximate form $G_2(t) \cong \exp(-\lambda t) G_2^{\text{static}}(t)$ [9]. Here, $G_2^{\text{static}}(t)$ is the static perturbation function for quadrupole interaction and λ is the relaxation frequency. In Ref. [7] it was shown that $\lambda = w$ for a jump model with stochastic reorientations of the EFG along the three cube directions. The form given above was shown in Ref. [10] to be an adequate approximation in the slow fluctuation regime.

Representative spectra measured at 1120 K for a light (Pr) and a heavy (Tm) lanthanide indide are compared in Fig. 1. Signals having ~100-ns period are from probe atoms on the A sublattices, with frequencies in agreement with previous measurements [11,12]. Damping is visibly greater for A-richer In_3Pr (top left) and for B-richer In_3Tm (bottom right). Spectra were fitted to determine the jump frequencies, with Arrhenius plots for In_3Pr and In_3Tm shown in Fig. 2. Straight lines represent results of fits of temperature dependences of jump frequencies at the A-richer (A) or B-richer (B) boundary compositions with $w = w_0 \exp(-Q/k_BT)$, in which Q is a jump-frequency activation enthalpy and w_0 is a frequency prefactor [13]. As can be seen, jump frequencies w_A at the A-richer boundary are greater than jump frequencies w_B at the B-richer boundary for In_3Pr whereas $w_A < w_B$ for In_3Tm.

About 25 Arrhenius plots similar to those in Fig. 2 have been measured for indides and fitted in the present and previous work. Activation enthalpies are in the range 0.54–1.75 eV and jump-frequency prefactors are in the range 1–100 THz. Detailed consideration of these activation enthalpies and prefactors will be presented elsewhere. Here, we emphasize general features of the observations by adopting the temperature at which the jump frequency is 10 MHz as a single measure summarizing diffusion behavior for each sample. These characteristic temperatures, designated as T_{10}, can be accurately determined from Arrhenius plots such as those shown in Fig. 2. Figure 3 shows a plot of inverse temperatures $1/k_BT_{10}$ for all samples as a function of lattice parameter at room temperature [11,14]. Closed and open symbols refer to A-richer and B-richer boundary compositions.

There is a striking difference between the heavy and the light lanthanides. For the heavy lanthanides Lu, Tm, Er, Ho, and Dy, inverse temperatures $1/k_BT_{10}$ at both boundaries can be seen to decrease gradually as the lattice parameter increases. On the contrary, inverse temperatures for the light lanthanides Pr, Ce, and La increase with increasing lattice parameter. These differences indicate that different diffusion mechanisms are active in the heavy and light lanthanides. Dashed lines drawn in Fig. 3 extrapolate trends from either diffusional domain into the other.

When $1/k_BT_{10}$ is greater at the A-richer boundary than at the B-richer boundary, $w_A > w_B$ and the ratio w_A/w_B is greater than 1, whereas $w_A/w_B < 1$ when the inverse temperature of the B-richer boundary is greater. Thus, the ratio of jump frequencies offers an alternative differentiation between behavior at the boundary compositions, with $w_A/w_B < 1$ for the heavy lanthanides and crossing over between Sm and Nd to $w_A/w_B > 1$ for the light lanthanides.

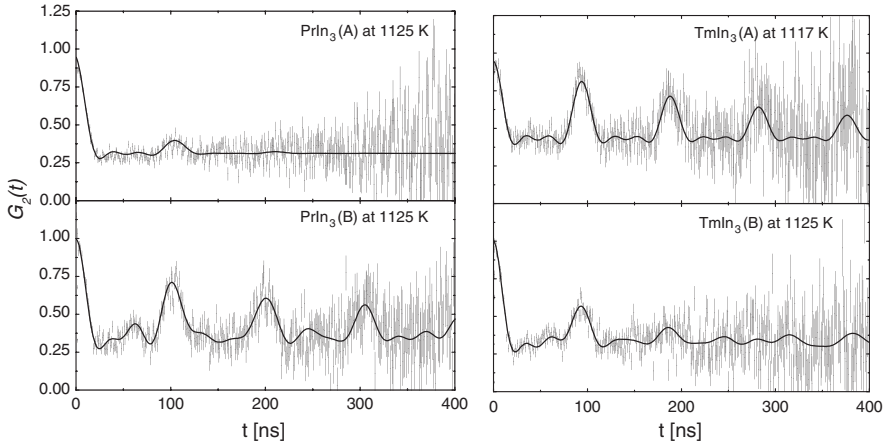

FIG. 1. PAC spectra of In_3Pr (left) and In_3Tm (right) measured at 1120 K. Top and bottom spectra were measured, respectively, for samples having In-richer (A) or In-poorer (B) boundary compositions.

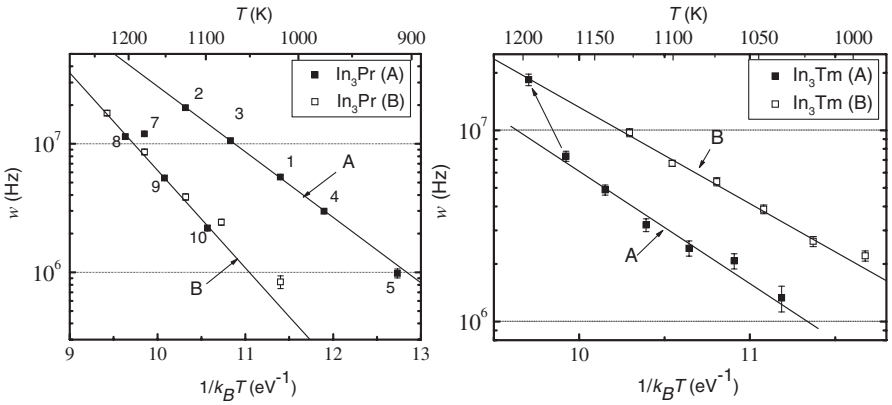

FIG. 2. Arrhenius plots of fitted jump frequencies for In_3Pr (left) and In_3Tm (right). Jump frequencies are greater for the In-richer (A) boundary composition in In_3Pr but for the In-poorer (B) composition in In_3Tm.

Diffusion is mediated by lattice vacancies in close-packed alloys of elements that have similar atomic radii, such as for rare-earth elements and indium [1]. In principle, either A- or B-sublattice vacancies, V_A or V_B, may be involved. A central result of this Letter is that the vacancy type that predominates in diffusion of probe atoms can be identified by the ratio w_A/w_B. In the absence of interactions among point defects, it can be shown that, at a given temperature, the mole fraction of V_A, $[V_A]$, must increase monotonically as the content of element A decreases, and similarly for V_B. As a consequence, $[V_A]$ is greater at the A-poorer (B) and $[V_B]$ is greater at the A-richer (A) boundary compositions. Since the overall jump frequency induced by a mechanism is proportional to the mole fraction of the relevant vacancy, one can conclude that diffusion in the heavy (or light) lanthanide indides is dominated by mechanisms involving V_A (or V_B).

We consider next the more likely detailed diffusion mechanisms. For a review of diffusion mechanisms in $L1_2$ phases, the reader is referred to Ref. [15] and references therein. In highly ordered phases, vacancy jumps that create lattice disorder in the form of antisite atoms are disfavored due to the energy cost. In the $L1_2$ structure, each A-site has 8 A-atom NN and 4 B-atom NN while each B-site has 12 A-atom NN. Thus, it is possible for V_A to diffuse by NN jumps on a connected A-sublattice without creating defects. This will be the dominant V_A-mediated diffusion mechanism for atoms on the A sublattice since other mechanisms involve creation of disorder. V_B, on the other hand, cannot make NN jumps without creating a defect. While a jump of V_B to another B site is conceivable (a ''long jump''), the activation enthalpy tends to be much greater due to the long jump distance [16]. More complex diffusion mechanisms involving NN jumps of V_B were already discussed in [5] (see also [15]), of which the simplest one involves only one B vacancy. This is the B-vacancy six-jump cycle mechanism, in which a B vacancy makes six successive jumps that first create and then eliminate three antisite atom defects [15]. Such jump sequences have been proposed for other binary compounds and are generally considered to be most important for well-ordered, near-stoichiometric phases, like those in the present study [1]. The above two mechanisms are illustrated in Fig. 4. Another mechanism that is possible for a single B vacancy is conversion of a B vacancy into an A vacancy and A-antisite atom complex via the reaction $V_B + A_A \leftrightarrow V_A + A_B$. This mechanism would appear to

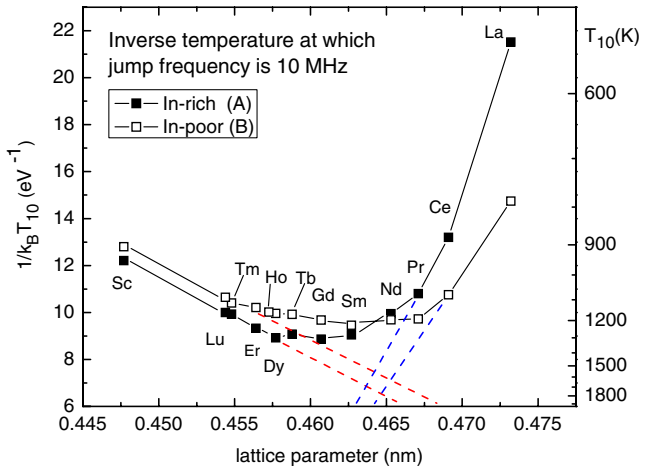

FIG. 3 (color online). Inverse temperatures $1/k_BT_{10}$ at which jump frequencies reach 10 MHz for In-richer (filled symbols) or In-poorer (open symbols) phase boundary compositions, plotted versus lattice parameters of the rare-earth indides. Dashed lines are extrapolations of trends for light and heavy lanthanide indides that illustrate changes in behavior attributed to different diffusion mechanisms.

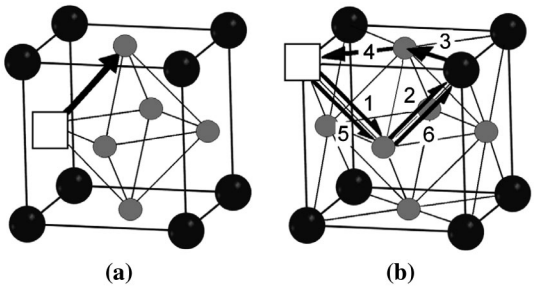

FIG. 4. Diffusion mechanisms in A_3B alloys having the $L1_2$ crystal structure. B atoms are at cube corners and A atoms at face centers. Arrows show vacancy jumps. (a) A-vacancy sublattice diffusion. (b) B-vacancy six-jump cycle (bent version).

allow simple A-sublattice vacancy diffusion to occur if the V_A could "escape" from the stationary antisite A_B defect. However, it can be shown that this mechanism will lead to $w_A > w_B$ only when there is significant binding between V_A and A_B, in which case V_A will be essentially restricted to local hops on the 12 A sites that neighbor the A_B antisite atom. Such a scenario would lead to two ensembles of PAC probes jumping on A sites at very different rates, which has never been observed in our measurements. Other mechanisms involve correlated motions of defect complexes such as a bound V_A-V_B pair. In spite of the complexity of the jump sequence, the B-vacancy six-jump cycle mechanism involves only an isolated B-vacancy defect and appears to be the most plausible one for the light lanthanides.

Inverse temperatures for In_3Sc were included in Fig. 3 because they appear to extrapolate trends for the heavy lanthanide indides to smaller lattice parameter. This shows that diffusion behavior is highly correlated with the lattice parameter and, indeed, may be controlled by it. The present measurements on indides stand in contrast to similar PAC studies on light and intermediate rare-earth stannides of La [7], Ce [17], and Sm and Gd [18], which have uniformly shown that $w_B > w_A$. Consequently, sublattice A-vacancy diffusion is the predominant diffusion mechanism in early lanthanide stannides, unlike in the indides. Apparently, chemical properties in the indides are such that defect formation and migration energies are near critical values that allow a small change in lattice parameter to trigger a changeover between diffusion mechanisms in the middle of the series.

Finally, it must be noted that the jump frequency is observed here for an impurity ^{111}Cd atom and not a host indium atom. Thus, jump frequencies of indium host atoms may of course differ [1,4]. However, conclusions about diffusion mechanisms based on differences in jump frequencies at boundary compositions remain valid for host and impurity tracers alike.

In summary, measurements were made of jump frequencies of Cd impurities on the A sublattice in highly ordered rare-earth indides A_3B having the $L1_2$ structure. Figure 3 shows that there is a smooth transition from $w_B/w_A > 1$ for the heavy lanthanide indides to $w_A/w_B > 1$ for the light lanthanides. For heavy lanthanide indides, it was shown that the predominant diffusion mechanism for atoms on the A sublattice involves V_A and is almost certainly sublattice A-vacancy diffusion. For the light lanthanide indides, the predominant mechanism must involve V_B, with the most likely candidate being the B-vacancy six-jump cycle mechanism. The change in diffusion behavior appears to be controlled by the lattice parameter. We are unaware of a previous study in which a similar change in diffusion mechanism was observed along a series of isostructural compounds.

This work was supported in part by the National Science Foundation under grant DMR 05-04843 (Metals Program) and by the Praveen Sinha Fund for Physics Research. Justin Ahn, Megan Lockwood, and Benjamin Norman helped with some of the measurements.

[1] H. Mehrer, *Diffusion in Solids: Fundamentals, Methods, Materials, Diffusion Controlled Processes* (Springer, Berlin, 2007).
[2] Wolfgang Püschl, Hiroshi Numakura, and Wolfgang Pfeiler, in *Alloy Physics*, edited by Wolfgang Pfeiler (Wiley-VCH, Weinheim, 2007), Chap. 5.
[3] Gero Vogl and Raimund Feldwisch, in *Diffusion in Condensed Matter*, edited by Jörg Kärger, Paul Heitjans, and Reinhold Haberlandt (Vieweg, Braunschweig, 1998), Chap. 2, p. 41.
[4] Jean Philibert, *Atom Movements: Diffusion and Mass Transport in Solids* (Les Editions de Physique, Les Ulis, 1991).
[5] Matthew O. Zacate, Aurélie Favrot, and Gary S. Collins, Phys. Rev. Lett. **92**, 225901 (2004); Matthew O. Zacate, Aurélie Favrot, and Gary S. Collins, Phys. Rev. Lett. **93**, 049903(E) (2004).
[6] G. S. Collins *et al.*, Defect and Diffusion Forum **237–240**, 195 (2005).
[7] Gary S. Collins *et al.*, Hyperfine Interact. **159**, 1 (2005).
[8] *Binary Alloy Phase Diagrams*, edited by T. B. Massalski, H. Okamoto, P. R. Subramanian, and Linda Kacprzak (ASM International, Materials Park, Ohio, 1990).
[9] A. Baudry and P. Boyer, Hyperfine Interact. **35**, 803 (1987).
[10] Matthew O. Zacate and William E. Evenson, Hyperfine Interact. **158**, 329 (2004).
[11] G. P. Schwartz and D. A. Shirley, Hyperfine Interact. **3**, 67 (1977).
[12] For In-poorer samples (B), signals with small amplitudes due to neighboring phases were fitted together with the dominant $L1_2$ signal. For In-richer samples (A), adjacent phases were indium metal that was molten at temperatures of measurement and gave a motionally averaged signal appearing as a time-independent offset.
[13] During measurement, some indide samples that were originally A-richer lost indium gradually through evaporation, eventually switching to the B-richer boundary composition. This is observed in Fig. 2 for points 8–10 in sequence of measurements on the initially A-rich sample of In_3Pr and for the last measurement on the A-rich sample in In_3Tm (see arrow).
[14] *Phase Diagrams of Indium Alloys and their Engineering Applications*, edited by C. E. T. White and H. Okamoto (ASM International, Materials Park, OH, 1992).
[15] M. Koiwa, H. Numakura, and S. Ishioka, Defect and Diffusion Forum **143–147**, 209 (1997).
[16] For example, in a recent simulation for Ni_3Al the activation enthalpy for a second NN jump was calculated to be 15 times greater than for a NN jump; Guo-Xiang Chen *et al.*, Physica (Amsterdam) **403B**, 3538 (2008).
[17] Benjamin Norman, undergraduate honors thesis, 2007 (unpublished).
[18] Megan Lockwood (unpublished).